THE JOURNAL OF PHYSICAL CHEMISTRY B

ARTICLE

pubs.acs.org/JPCB

Kinetic Analysis of Demetalation of Synthetic Zinc Cyclic Tetrapyrroles Possessing an Acetyl Group at the 3-Position: Effects of Tetrapyrrole Structures and Peripheral Substitution

Yoshitaka Saga,* Ryosuke Miura, Kana Sadaoka, and Yuki Hirai

Department of Chemistry, Faculty of Science and Engineering, Kinki University, Higashi-Osaka, Osaka 577-8502, Japan

ABSTRACT: Demetalation of three synthetic zinc cyclic tetrapyrroles that possess identical peripheral substituents, zinc methyl bacteriopyropheophorbide *a* (zinc bacteriochlorin **1**), zinc methyl 3-devinyl-3-acetyl-pyropheophorbide *a* (zinc chlorin **2**), and zinc methyl 3-devinyl-3-acetyl-protopyropheophorbide *a* (zinc porphyrin **3**), was kinetically analyzed under acidic conditions to examine the effects of macrocyclic structures on demetalation without peripheral substitution effects. Zinc bacteriochlorin **1** exhibited much slower demetalation kinetics than zinc chlorin **2** and zinc porphyrin **3**. These results indicate that the bacteriochlorin skeleton provides significant resistance to the removal of the central metal from the tetrapyrrole ligand. Comparison of demetalation kinetics of 3-acetyl zinc complexes **2** and **3** with that of 3-vinyl zinc complexes under the same reaction condition demonstrated that the relative ratio (5.0×10^{-2}) of the demetalation rate constant of the 3-acetyl zinc chlorin **2** to that of the corresponding 3-vinyl zinc chlorin **4** resembled the case of the 3-acetyl zinc porphyrin **3** to the 3-vinyl zinc porphyrin **5** (the relative ratio was 6.8×10^{-2}). These suggest that the electron-withdrawing 3-acetyl group slows down the demetalation from the tetrapyrrole ligands more than the 3-vinyl group and that the 3-acetyl effect is analogous in both chlorin and porphyrin π-systems.

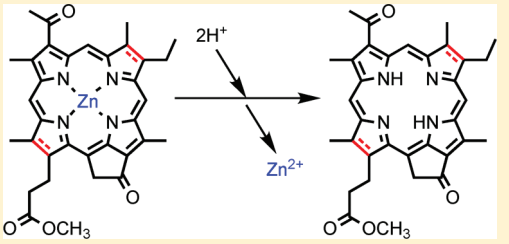

INTRODUCTION

Cyclic tetrapyrroles, such as porphyrin, chlorin, and bacteriochlorin, are biologically important moieties in nature.[1−3] Porphyrin is the functional core of heme, which is a key cofactor in enzymes and electron-transferring and oxygen-transporting proteins. Chlorin and bacteriochlorin, which are 17,18-dihydroporphyrin and 7,8,17,18-tetrahydroporphyrin, respectively, are the fundamental moieties of naturally occurring photosynthetic pigments. Porphyrin-type pigments are also present in photosynthetic organisms; chlorophyll(Chl)s *c* function as light-harvesting pigments in chromophyte algae and some prokaryotes,[4] and protochlorophyllide *a* is one crucial biosynthetic intermediate in photosynthetic organisms.[5] Most of these natural cyclic tetrapyrrole molecules possess a central metal in their π-macrocycles.

Removal of a central metal from cyclic tetrapyrrole molecules is an important reaction in biological systems. Chls release central magnesium in the early process of in vivo Chl degradation.[6−9] Moreover, demetalation of Chls and bacteriochlorophyll(BChl)s could be a key reaction in the formation of the primary electron acceptor in photosystem II-type reaction centers. From these viewpoints, demetalation of cyclic tetrapyrrole molecules has attracted much attention. Demetalation reactions of photosynthetic cyclic tetrapyrrole pigments have been extensively studied from the reports of Mackinney and Joslyn in the early 1940s.[10−24] Mazaki et al. reported the detailed demetalation properties of Chls *a*, *b*, and their epimers (Chls *a*′ and *b*′, respectively).[15,16] Kobayashi et al. studied in vitro demetalation of naturally occurring Zn-BChl *a*,[17,18] which was discovered in a purple photosynthetic bacterium, *Acidiphilium rubrum*.[25−28] We recently reported the demetalation properties of natural (B)Chls, such as BChls *c*, *d*, and *e* in green sulfur photosynthetic bacteria[19,20] and Chl *d* in a cyanobacterium *Acaryochloris marina*,[21] as well as synthetic chlorophyllous pigments.[22−24]

Some of these previous reports revealed that peripheral substituents in cyclic tetrapyrrole molecules affected their demetalation properties.[10,11,15,19−21,23,24] In contrast, few reports are available on the effects of macrocyclic structures of cyclic tetrapyrrole molecules on the removal of central metal from tetrapyrrole ligands.[17,18,22] Kobayashi et al. compared the demetalation kinetics of Mg-BChl *a*, Zn-BChl *a*, Mg-Chl *a*, and Zn-Chl *a*, concluding that Mg- and Zn-BChl *a* exhibited slower removal of central metal than Mg- and Zn-Chl *a*.[17,18] In comparison between BChl *a* and Chl *a*, however, the influences of the peripheral substituents in these pigments cannot be ruled out, since the substituent at the 3-position of BChl *a* is different from that of Chl *a*; BChl *a* and Chl *a* have acetyl and vinyl groups, respectively, at this position. Therefore, direct comparison of the demetalation properties among cyclic tetrapyrrole molecules possessing the same peripheral substituents is necessary to unravel the effects of macrocyclic structures without substitution effects. We preliminarily reported the demetalation kinetics of 3-vinyl zinc chlorin (zinc methyl pyropheophorbide *a*, **4** in Figure 1B) and porphyrin (zinc methyl protopyropheophorbide *a*, **5** in Figure 1B), both of which possessed identical peripheral substituents.[22] In the present study,

Received: July 11, 2011
Revised: September 2, 2011
Published: September 22, 2011

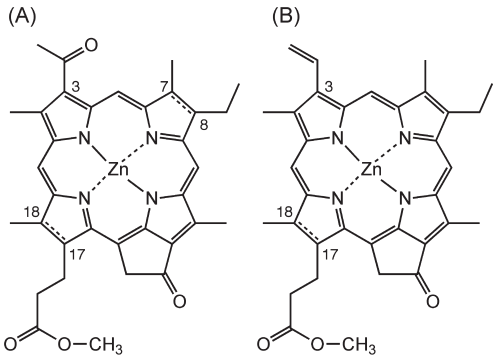

	C7–C8	C17–C18
1	single bond	single bond
2	double bond	single bond
3	double bond	double bond

	C17–C18
4	single bond
5	double bond

Figure 1. (A) Molecular structures of zinc methyl bacteriopyropheophorbide *a* (zinc bacteriochlorin **1**), zinc methyl 3-devinyl-3-acetyl pyropheophorbide *a* (zinc chlorin **2**), and zinc methyl 3-devinyl-3-acetyl protopyropheophorbide *a* (zinc porphyrin **3**). (B) Molecular structures of zinc methyl pyropheophorbide *a* (**4**), and zinc methyl protopyropheophorbide *a* (**5**).

we examine the demetalation properties of three types of 3-acetylated cyclic tetrapyrrole molecules; only their macrocyclic structures are different. The molecular structures of the three cyclic tetrapyrroles used in this study are shown in Figure 1A. Zinc methyl bacteriopyropheophorbide *a* (denoted as zinc bacteriochlorin **1**), which is a good model compound of BChl *a* in photosynthetic bacteria, possesses the bacteriochlorin macrocycle. Zinc methyl 3-devinyl-3-acetyl pyropheophorbide *a* (denoted as zinc chlorin **2**) has a chlorin macrocycle as the photofunctional moiety. Zinc methyl 3-devinyl-3-acetyl protopyropheophorbide *a* (denoted as zinc porphyrin **3**) has the same peripheral substituents as **1** and **2**, but double bonds in both 7C−8C and 17C−18C. Comparison of the demetalation properties among compounds **1**−**3** allows us to study the effects of macrocyclic structures on demetalation without peripheral substitution effects. We can also discuss the effect of the 3-acetyl group on the demetalation properties of chlorin and porphyrin molecules by comparing the results of **2** and **3** in this study with those of the 3-vinyl chlorin and porphyrin derivatives (**4** and **5**, respectively).[22]

EXPERIMENTAL SECTION

Apparatus. Visible absorption spectra were measured with a Shimadzu UV-2450 spectrophotometer, where the reaction temperature was regulated with a Shimadzu thermo-electric temperature-controlled cell holder TCC-240A. High-performance liquid chromatography (HPLC) was performed with a Shimadzu LC-20AT pump and an SPD-M20A or SPD-20AV detector. Mass spectra were measured with a JEOL JMS700 spectrometer; *m*-nitrobenzyl alcohol was used as a matrix.

Materials. Three zinc cyclic tetrapyrroles, zinc methyl bacteriopyropheophorbide *a* (**1**), zinc methyl 3-devinyl-3-acetyl pyropheophorbide *a* (**2**), and zinc methyl 3-devinyl-3-acetyl protopyropheophorbide *a* (**3**) were synthesized according to previous reports.[22,29,30] Compound **1** was synthesized through four steps from BChl *a*, which was extracted from a purple photosynthetic bacterium *Rhodobacter sphaeroides*.[29] Compounds **2** and **3** were synthesized from Chl *a* as follows. Methyl pyropheophorbide *a*

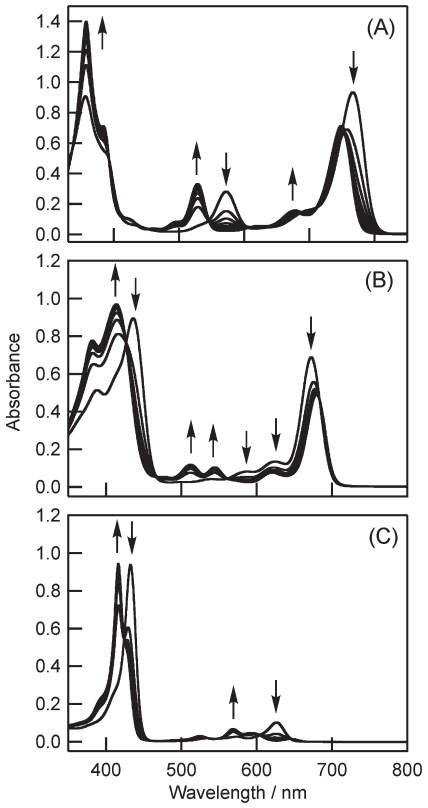

Figure 2. Spectral changes of zinc bacteriochlorin **1** (A), zinc chlorin **2** (B), and zinc porphyrin **3** (C) in acetone/water (10/1, vol/vol) at the proton concentration of 3.6×10^{-2}, 1.2×10^{-2}, and 1.2×10^{-2} M, respectively, at 25 °C. **1**: spectra from 0 to 250 min at 10-min intervals. **2**: spectra from 0 to 100 min at 10-min intervals. **3**: spectra from 0 to 120 min at 10-min intervals. The arrows show the direction of the absorbance changes.

was synthesized through three steps from Chl *a*, and the 3-vinyl group was converted to the acetyl group *via* the hydroxyethyl group to afford methyl 3-devinyl-3-acetyl pyropheophorbide *a*. A methanol solution saturated with $Zn(CH_3COO)_2 \cdot 2H_2O$ was added to a dichloromethane solution of methyl 3-devinyl-3-acetyl pyropheophorbide *a*, and the solution was stirred at room temperature for ca. 2 h to afford zinc methyl 3-devinyl-3-acetyl pyropheophorbide *a* (**2**). The resulting **2** was reacted with 2,3-dichloro-5,6-dicyano-1,4-benzoquinone (1 equiv) in distilled acetone to give zinc methyl 3-devinyl-3-acetyl protopyropheophorbide *a* (**3**).[22,29,30] Zinc complexes **1**−**3** were purified by reverse-phase HPLC.

Characteristic spectral data of **1**−**3** are described as follows (see also ref.[29]): zinc methyl bacteriopyropheophorbide *a* (**1**): UV−vis (acetone) λ_{max} = 764 (relative intensity, 1.00), 563 (0.28), 388 (0.56), 353 (0.92). MS (FAB): found: *m*/*z* 628.2, calcd for $C_{34}H_{36}N_4O_4Zn$ (M^+), 628.2. Zinc methyl 3-devinyl-3-acetyl pyropheophorbide *a* (**2**): UV−vis (acetone) λ_{max} = 668 (relative intensity, 0.73), 620 (0.13), 579 (0.08), 533 (0.04), 433 (1.00). MS (FAB): found: *m*/*z* 626.2, calcd for $C_{34}H_{34}N_4O_4Zn$ (M^+), 626.2. Zinc methyl 3-devinyl-3-acetyl protopyropheophorbide *a* (**3**): UV−vis (acetone) λ_{max} = 621 (relative intensity, 0.11), 569 (0.03), 429 nm (1.00). MS (FAB): found: *m*/*z* 624.2, calcd for $C_{34}H_{32}N_4O_4Zn$ (M^+), 624.2.

Measurements of Demetalation Kinetics. Measurements of demetalation kinetics of synthetic zinc complexes **1**−**3** were

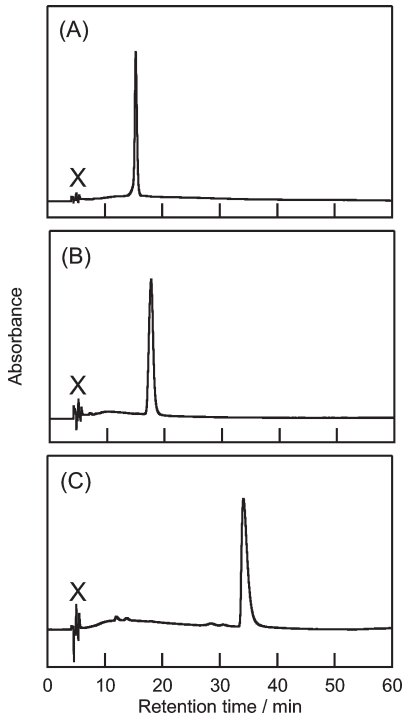

Figure 3. HPLC elution patterns of reaction products of zinc bacteriochlorin **1** (A), zinc chlorin **2** (B), and zinc porphyrin **3** (C) in acetone/water (10/1, vol/vol) at the proton concentration of 3.6×10^{-2} M at 25 °C after incubation for 120, 30, and 30 min, respectively. The reaction products were eluted on a reverse-phase HPLC column $5C_{18}$-AR-II (6.0 mm i.d. × 250 mm) with a guard column $5C_{18}$-AR-II (4.6 mm i.d. × 10 mm) using methanol as an eluent at a flow rate of 1.0 mL min^{-1}. Chromatograms were recorded at 357, 411, and 417 nm for reaction products of **1**, **2**, and **3**, respectively. The signals denoted by × were due to the direct injection of reaction solvents.

performed in the similar procedure to previous reports.[15−17,19−24] A 3 mL acetone solution of **1**−**3** (Soret absorbance =1.0) was mixed with 0.28 mL of distilled water. In kinetic analysis of demetalation processes, 20 μL of aqueous hydrochloric acid for volumetric analysis (Wako Pure Chemical Industries, Ltd., Japan) was added to the solutions, and absorbance at the Soret or Q_y peak position of zinc complexes **1**−**3** was measured under the control of reaction temperatures between 15 and 35 °C.

Pigment Analysis after Demetalation. After demetalation reactions, the solutions were directly analyzed on a reverse-phase HPLC column $5C_{18}$-AR-II (6.0 mm i.d. × 250 mm) with a guard column $5C_{18}$-AR-II (4.6 mm i.d. × 10 mm) using methanol as an eluent at a flow rate of 1.0 mL min^{-1}.

RESULTS

The demetalation properties of synthetic cyclic tetrapyrroles **1**−**3** were examined in acidic aqueous acetone. Figure 2 shows the spectral changes of **1**−**3** during the demetalation processes in acetone/water (10/1, vol/vol) at the proton concentrations of 3.6×10^{-2}, 1.2×10^{-2}, and 1.2×10^{-2} M at 25 °C. In this solution, zinc bacteriochlorin **1** possessed Soret, Q_x, and Q_y bands at 356, 572, and 767 nm, respectively. The Q_x and Q_y absorption bands decreased under the acidic condition, accompanying new absorption bands at 529 and 749 nm. The 529- and 749-nm bands were ascribable to the Q_x and Q_y bands, respectively, of the demetalation form of zinc bacteriochlorin **1**. The absorbance in

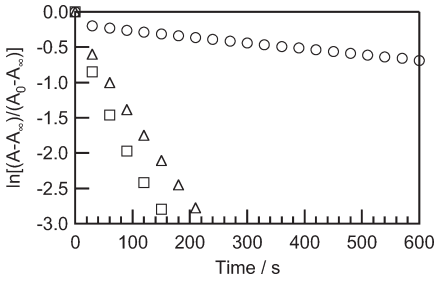

Figure 4. Kinetic plots for demetalation of zinc bacteriochlorin **1** (open circle), zinc chlorin **2** (open square), and zinc porphyrin **3** (open triangle) in acetone/water (10/1, vol/vol) at the proton concentration of 3.6×10^{-2} M at 25 °C. Absorbance changes were monitored at 767, 436, and 433 nm for **1**, **2**, and **3**, respectively. A_0, A, and A_∞ are absorbance of **1**−**3** at the onset of the measurement, at time t, and at the complete demetalation, respectively.

the Soret region of **1** increased by incubation. Isosbestic points were clearly observed at 392, 410, 437, 453, 546, 606, 687, 711, and 752 nm during the demetalation reaction.

Zinc chlorin **2** showed Soret and Q_y bands at 436 and 672 nm, respectively, in aqueous acetone. The Soret band of zinc chlorin **2** at 436 nm decreased and a new Soret band, which was ascribable to the demetalation form of zinc chlorin **2**, appeared at 414 nm. The 672-nm Q_y band of **2** was also decreased and shifted to a longer wavelength. Small absorption bands between 500 and 600 nm gradually changed, and isosbestic points could also be observed at 427, 467, 561, and 684 nm during the demetalation reactions of zinc chlorin **2**.

In the case of zinc porphyrin **3**, the 433-nm Soret band decreased with the appearance of a new band at 417 nm. The new 417-nm band was ascribable to the Soret band of the demetalation form of **3**. Small absorption bands between 500 and 650 nm gradually changed through the demetalation reaction of **3**. Isosbestic points were also present at 424, 460, 535, 549, and 604 nm during the demetalation process.

The reaction products of **1**, **2**, and **3** by incubation for 120, 30, and 30 min, respectively, in acetone/water (10/1, vol/vol) at the proton concentration of 3.6×10^{-2} M at 25 °C were analyzed by reverse-phase HPLC (Figure 3). The main product after the demetalation reaction of zinc bacteriochlorin **1** was eluted at 15 min. This product had Soret, Q_x, and Q_y bands at 357, 531, and 749 nm, respectively, in the HPLC eluent and was assigned to a demetalation compound of **1** (methyl bacteriopyropheophorbide *a*).

HPLC analysis of the reaction products of zinc chlorin **2** showed that the product eluted at 18 min, whose Soret and Q_y bands were positioned at 411 and 682 nm in the HPLC eluent, was predominantly formed. This product was assigned to the demetalation form of **2**: methyl 3-devinyl-3-acetyl pyropheophorbide *a*. A slight fraction, which would be ascribed to the byproduct through the reaction, was observed at 7 min. In the case of **3**, the main product eluted at 34 min, which exhibited the Soret band at 417 nm in the HPLC eluent, was ascribable to demetalated **3**, namely methyl 3-devinyl-3-acetyl protopyropheophorbide *a*. Slight fractions at 12, 14, 29, and 31 min in Figure 3C were attributable to the byproduct through the demetalation reaction of **3**. These analyses indicate that zinc complexes **1**−**3** were predominantly converted to the corresponding demetalation forms with only slight side reaction under the present condition. It should be noted that drifts were observed around 10−20 min in the chromatograms in Figure 3A−C, probably

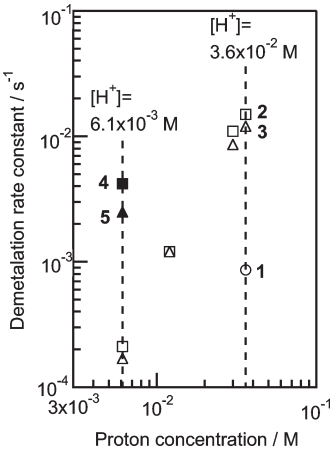

Figure 5. Demetalation rate constants of zinc bacteriochlorin **1** (open circle), zinc chlorin **2** (open square), and zinc porphyrin **3** (open triangle) in acetone/water (10/1, vol/vol) at 25 °C. Demetalation rate constants of **4** (closed square) and **5** (closed triangle) determined in the previous study[22] were also plotted.

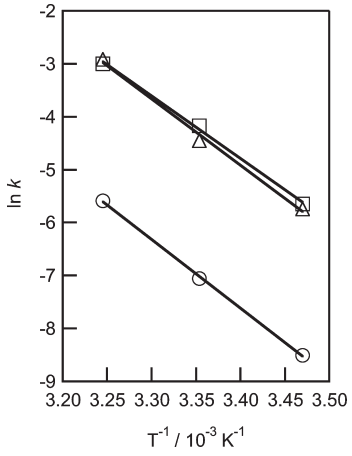

Figure 6. Arrhenius plots over temperature range of 15−35 °C for the reduction rate constants of zinc bacteriochlorin **1** (open circle), zinc chlorin **2** (open square), and zinc porphyrin **3** (open triangle) in acetone/water (10/1, vol/vol) at the proton concentration of 3.6×10^{-2} M.

because of direct injection of diluted solutions of reaction products.

The demetalation reactions were quantitatively analyzed by monitoring the absorbance changes at the Q_y peak position for zinc bacteriochlorin **1** and those at the Soret peak positions of zinc chlorin **2** and zinc porphyrin **3**. The time courses of the absorbance of **1**−**3** incubated in acetone/water (10/1, vol/vol) at the proton concentration of 3.6×10^{-2} M at 25 °C are shown in Figure 4. The logarithm of the absorbance in the demetalation reactions of **1**−**3** showed linear time dependence, indicating that the demetalation reactions of **1**−**3** can be regarded as pseudo-first-order reactions. This is in line with the reaction condition in which the proton concentration was much higher than the concentration of synthetic cyclic tetrapyrroles **1**−**3** ($<10^{-5}$ M). The kinetic plots in Figure 4 were slightly shifted from zero point. This was mainly ascribable to the lag to equilibrium in reaction solutions after addition of aqueous hydrochloric acid, but the possibility that the initial stage of the reaction might be somewhat different from the later stage cannot be ruled out. Reaction rate constants *k*s of the demetalation under the present condition were obtained by fitting the time courses of the absorbance of **1**−**3** to the following kinetic equation:

$$\ln(A - A_\infty)/(A_0 - A_\infty) = -kt$$

where A_0, A, and A_∞ are the absorbance at the onset of the measurement, at time t, and at the complete demetalation, respectively. The demetalation rate constants of **1**, **2**, and **3** at 25 °C, which were estimated from the kinetic plots in this study, as well as those of 3-vinyl compounds **4** and **5** in the previous study[22] are shown in Figure 5. The demetalation rate constants of **1**−**3** are the averages of more than three independent measurements, and their standard deviations were less than 9% of the average *k*-values, respectively. The demetalation rate constant of zinc bacteriochlorin **1** was 17- and 14-times smaller than those of zinc chlorin **2** and zinc porphyrin **3**, respectively, at the proton concentration of 3.6×10^{-2} M. The comparison of the demetalation kinetics between **2** and **3** indicated that the demetalation rate constant of **3** was 1.3-times smaller than that of **2**, which was in line with previous work on 3-vinyl zinc chlorin **4** and 3-vinyl zinc porphyrin **5**.[22]

The demetalation rate constants of zinc chlorin **2** and zinc porphyrin **3** were compared with those of **4** and **5** (Figure 5) to examine the effect of the 3-acetyl group on the demetalation of zinc cyclic tetrapyrroles. The demetalation rate constant of **3** was 1.2-times smaller than that of **2** at the proton concentration of 6.1×10^{-3} M. The relative ratio of the demetalation rate constant of 3-acetyl zinc chlorin **2** to that of 3-vinyl zinc chlorin **4**, $k(\mathbf{2})/k(\mathbf{4})$, was 5.0×10^{-2}. The value was analogous to the case of 3-acetyl and 3-vinyl zinc porphyrins; the relative ratio $k(\mathbf{3})/k(\mathbf{5})$ was 6.8×10^{-2}. These indicate that the 3-acetyl group gives more tolerance to the demetalation of cyclic tetrapyrroles than the 3-vinyl group, and the effect of the 3-acetyl group is similar in both chlorin and porphyrin macrocycles.

The temperature dependence of the demetalation rate constants of **1**−**3** at the proton concentration of 3.6×10^{-2} M was examined between 15 and 35 °C at 10 °C intervals. The demetalation kinetics of **1**−**3** slowed down with decrease of the reaction temperature. The demetalation rate constants of **1**−**3** in this temperature range were estimated by fitting the time course of the absorbance to the above kinetic equation, since the demetalation reactions are also regarded as pseudo-first-order reactions. The temperature-dependent demetalation rate constants of **1**−**3** gave the Arrhenius plots shown in Figure 6. As a result, the activation energies of the demetalation of **1**, **2**, and **3** were estimated to be 108, 98, and 104 kJ mol^{-1}, respectively. The order of the activation energies of demetalation for the cyclic tetrapyrroles was **1** (zinc bacteriochlorin) > **3** (zinc porphyrin) > **2** (zinc chlorin).

DISCUSSION

Comparison of the demetalation properties among zinc bacteriochlorin **1**, zinc chlorin **2**, and zinc porphyrin **3**, all of which possessed identical peripheral substituents, clearly demonstrated the effects of macrocyclic structures on the removal of central metal from cyclic tetrapyrrole ligands. Slower demetalation kinetics of bacteriochlorin-type molecules than that of chlorin-type molecules was reported using naturally occurring BChl *a* and Chl *a*,[17,18] but the effects of the 3-substituents in these pigments were not ruled out in the comparison of these natural pigments. Our study clearly revealed that the bacteriochlorin skeleton was responsible for high resistance to demetalation. The porphyrin

macrocycle also provided more resistance to demetalation than the chlorin macrocycle, but the effect was much smaller than that of the bacteriochlorin macrocycle.

Such several factors as the electron densities of core nitrogen atoms, electronic states and flexibility of π-macrocycles could cause differences of demetalation kinetics among the cyclic tetrapyrrole molecules. The electron densities of pyrrole nitrogen atoms in macrocycles are crucial factors for the removal of central metal from tetrapyrrole ligand, since the electrophilic attack of protons to the nitrogen atoms leads to the demetalation of cyclic tetrapyrroles. Previous ^{15}N NMR studies of BChl *a*[31,32] and Chl *a*[33] indicated lower-field shifts of four nitrogen atoms in BChl *a* (~190−260 ppm) than those of Chl *a* (~160−220 ppm), implying decrease of the electron densities of the core nitrogen atoms in BChl *a* compared with those of Chl *a*. Such changes of the electronic states of nitrogens in the macrocycle induce the structure-dependent demetalation properties observed in the present study.

The flexibility of the macrocyclic planes also affected the demetalation properties of the cyclic tetrapyrrole molecules. Our study indicated that flexible zinc bacteriochlorin **1** exhibited slower demetalation kinetics than rather rigid zinc chlorin **2** and zinc porphyrin **3**, although the order of demetalation rate constants of **1**−**3** did not correspond with that of their flexibility. Demetalation reactivity of cyclic tetrapyrrole molecules cannot be easily explained in terms of the macrocyclic flexibility, since several effects would be complexly responsible for their demetalation reactivity. Further detailed studies will be required to unravel effects of the flexibility of cyclic tetrapyrroles on demetalation reactivity thoroughly. It is worthy noting that a recent report on metal insertion to porphyrinoids suggested that the macrocycle rigidity as well as the electronic states of cyclic tetrapyrroles changed the chelating abilities of porphyrinoids.[34]

The comparison of the present results on zinc chlorin **2** and zinc porphyrin **3** with our previous results on the corresponding 3-vinyl compounds (**4** and **5**, respectively)[22] enables us to clearly unravel the effect of the 3-acetyl group of the cyclic tetrapyrrole on demetalation. The 3-acetyl group provided larger resistance to the removal of central zinc from the chlorin and porphyrin ligands than the 3-vinyl group. This originates from the electron-withdrawing ability of the 3-acetyl group. We demonstrated that the presence of the electron-withdrawing formyl groups in the A- and B-rings of the chlorin macrocycle induces slow demetalation kinetics.[19−21,23,24] The 3-acetyl effect on the demetalation kinetics in the present study is qualitatively in line with such substitution effects. The relative ratio of the demetalation rate constants of the 3-acetyl porphyrin **3** to the 3-vinyl porphyrin **5** was analogous to that of the 3-acetyl chlorin **2** to the 3-vinyl chlorin **4**, suggesting that the electron-withdrawing 3-acetyl group in the porphyrin skeleton affected the demetalation properties in a similar manner to that in the chlorin skeleton. Significant resistance to the demetalation of natural BChl *a* reported by Kobayashi et al.[17,18] reflects the combination of the effect of bacteriochlorin macrocycle with the 3-acetyl effect.

CONCLUSION

This study directly indicated that bacteriochlorin macrocycle provided much higher resistance to the removal of central metal from the cyclic tetrapyrrole ligand than chlorin and porphyrin macrocycles. This study also revealed that the 3-acetyl group contributed to slower demetalation kinetics in both chlorin and porphyrin π-systems, and the substitution from the vinyl to the acetyl group at the 3-position gave similar effects in both π-macrocycles. The tolerance of BChl *a* to demetalation compared with other naturally occurring chlorophyllous pigments such as Chl *a* is ascribable to both effects of the macrocyclic structure and the 3-acetyl group.

AUTHOR INFORMATION

Corresponding Author

*Phone: +81-6-6730-5880. Fax: +81-6-6723-2721. E-mail: saga@chem.kindai.ac.jp.

ACKNOWLEDGMENT

This work was partially supported by a Grant-in-Aid for Scientific Research (C) (No. 23550201) from the Japan Society for the Promotion of Science.

REFERENCES

(1) Smith, K. M., Ed. *Porphyrins and Metalloporphyrins*; Elsevier: Amsterdam, 1976.

(2) Kadish, K. M., Smith, K. M., Guilard, R., Eds. *Porphyrin Handbook*, Vol. 4; Academic Press: San Diego, CA, 2000.

(3) Grimm, B., Porra, R. J., Rüdiger, W., Scheer, H., Ed. *Chlorophylls and Bacteriochlorophylls: Biochemistry, Biophysics, Functions and Applications*; Springer: Dordrecht, the Netherlands, 2006.

(4) Zapata, M.; Garrido, J. L.; Jeffrey, S. W. In *Chlorophylls and Bacteriochlorophylls: Biochemistry, Biophysics, Functions and Applications*; Grimm, B., Porra, R. J., Rüdiger, W., Scheer, H., Ed.; Springer: Dordrecht, the Netherlands, 2006; pp 39−53.

(5) Rüdiger, W. In *Chlorophylls and Bacteriochlorophylls: Biochemistry, Biophysics, Functions and Applications*; Grimm, B., Porra, R. J., Rüdiger, W., Scheer, H., Ed.; Springer: Dordrecht, the Netherlands, 2006; pp 189−200.

(6) Kräutler, B.; Matile, P. *Acc. Chem. Res.* **1999**, *32*, 35–43.

(7) Kräutler, B.; Hörtensteiner, S. In *Chlorophylls and Bacteriochlorophylls: Biochemistry, Biophysics, Functions and Applications*; Grimm, B., Porra, R. J., Rüdiger, W., Scheer, H., Ed.; Springer: Dordrecht, the Netherlands, 2006; pp 237−260.

(8) Hörtensteiner, S. *Annu. Rev. Plant Biol.* **2006**, *57*, 55–77.

(9) Kräutler, B. *Photochem. Photobiol. Sci.* **2008**, *7*, 1114–1120.

(10) Mackinney, G.; Joslyn, M. A. *J. Am. Chem. Soc.* **1940**, *62*, 231–232.

(11) Mackinney, G.; Joslyn, M. A. *J. Am. Chem. Soc.* **1941**, *63*, 2530–2531.

(12) Schanderl, S. H.; Chichester, C. O.; Marsh, G. L. *J. Org. Chem.* **1962**, *27*, 3865–3868.

(13) Rosoff, M.; Aron, C. *J. Phys. Chem.* **1965**, *69*, 21–24.

(14) Berezin, B. D.; Drobysheva, A. N.; Karmanova, L. P. *Russ. J. Phys. Chem.* **1976**, *50*, 720–723.

(15) Mazaki, H.; Watanabe, T. *Bull. Chem. Soc. Jpn.* **1988**, *61*, 2969–2970.

(16) Mazaki, H.; Watanabe, T.; Takahashi, T.; Struck, A.; Scheer, H. *Bull. Chem. Soc. Jpn.* **1992**, *65*, 3212–3214.

(17) Kobayashi, M.; Yamamura, M.; Akiyama, M.; Kise, H.; Inoue, K.; Hara, M.; Wakao, N.; Yahara, K.; Watanabe, T. *Anal. Sci.* **1998**, *14*, 1149–1152.

(18) Kobayashi, M.; Akiyama, M.; Yamamura, M.; Kise, H.; Wakao, N.; Ishida, N.; Koizumi, M.; Kano, H.; Watanabe, T. *Z. Phys. Chem.* **1999**, *213*, 207–214.

(19) Saga, Y.; Hirai, Y.; Tamiaki, H. *FEBS Lett.* **2007**, *581*, 1847–1850.

(20) Hirai, Y.; Tamiaki, H.; Kashimura, S.; Saga, Y. *Photochem. Photobiol.* **2009**, *85*, 1140–1146.

(21) Hirai, Y.; Tamiaki, H.; Kashimura, S.; Saga, Y. *Photochem. Photobiol. Sci.* **2009**, *8*, 1701–1707.

(22) Saga, Y.; Hojo, S.; Hirai, Y. *Bioorg. Med. Chem.* **2010**, *18*, 5697–5700.
(23) Hirai, Y.; Kashimura, S.; Saga, Y. *Photochem. Photobiol.* **2011**, *87*, 302–307.
(24) Hirai, Y.; Sasaki, S.; Tamiaki, H.; Kashimura, S.; Saga, Y. *J. Phys. Chem. B* **2011**, *115*, 3240–3244.
(25) Wakao, N.; Yokoi, N.; Isoyama, N.; Hiraishi, A.; Shimada, K.; Kobayashi, M.; Kise, H.; Iwaki, M.; Itoh, S.; Takaichi, S.; Sakurai, Y. *Plant Cell Physiol.* **1996**, *37*, 889–893.
(26) Kobayashi, M.; Akiyama, M.; Kise, H.; Takaichi, S.; Watanabe, T.; Shimada, K.; Iwaki, M.; Itoh, S.; Ishida, N.; Koizumi, M.; Kano, H.; Wakao, N.; Hiraishi, A. *Photomed. Photobiol.* **1998**, *20*, 75–80.
(27) Wakao, N.; Hiraishi, A.; Shimada, K.; Kobayashi, M.; Takaichi, S.; Iwaki, M.; Itoh, S. In *The Phototrophic Prokaryotes*; Peschek, G. A., Loffelhardt, W., Schmetterer, G., Ed.; Plenum Publishing: New York, 1999; pp745−750.
(28) Kobayashi, M.; Akiyama, M.; Kise, H.; Watanabe, T. In *Chlorophylls and Bacteriochlorophylls: Biochemistry, Biophysics, Functions and Applications*; Grimm, B., Porra, R. J., Rüdiger, W., Scheer, H., Ed.; Springer: Dordrecht, the Netherlands, 2006; pp 55−66.
(29) Tamiaki, H.; Yagai, S.; Miyatake, T. *Bioorg. Med. Chem.* **1998**, *6*, 2171–2178.
(30) Tamiaki, H.; Watanabe, T.; Miyatake, T. *J. Porphyrins Phthalocyanines* **1999**, *3*, 45–52.
(31) Limantara, L.; Kurimoto, Y.; Furukawa, K.; Shimamura, T.; Utsumi, H.; Katheder, I.; Scheer, H.; Koyama, Y. *Chem. Phys. Lett.* **1995**, *236*, 71–77.
(32) Egorova-Zachernyuk, T.; van Rossum, B.; Erkelens, C.; de Groot, H. *Magn. Reson. Chem.* **2008**, *46*, 1074–1083.
(33) Boxer, S. G.; Closs, G. L.; Katz, J. J. *J. Am. Chem. Soc.* **1974**, *96*, 7058–7066.
(34) Orzel, L.; Kania, A; Rutkowska-Zbik, D.; Susz, A.; Stochel, G.; Fiedor, L. *Inorg. Chem.* **2010**, *49*, 7362–7371.